https://doi.org/10.5194/essd-2025-330
Preprint. Discussion started: 24 July 2025

Open Access Earth System Science Data Discussions

A High-Resolution, Long-Term Global Radar-Based Above-Ground Biomass Dataset from 1993 to 2020

Liu Guohua[1,2], Ciais Philippe[3], Tao Shengli[4], Yang Hui[4], and Bastos Ana[1,2]

[1]Leipzig University, Institute for Earth System Science and Remote Sensing, 04103 Leipzig, Germany
[2]Max Planck Institute for Biogeochemistry, 07745 Jena, Germany
[3]Laboratoire Sciences du Climat et de l'Environnement, 91191 Paris, France
[4]College of Urban and Environmental Sciences, Peking University, 100871 Beijing, China

Correspondence: Guohua Liu (guohua.liu@uni-leipzig.de)

Abstract.

Understanding global carbon dynamics and budgets under climate change, land-use shifts, and increasing disturbances remains challenging due to the limitations of existing coarse spatial resolution and short-term or discontinuous biomass datasets. In this study, we generated a new global annual above-ground biomass carbon (AGC) dataset at 8 km spatial resolution from 1993 to 2020. This dataset is derived from satellite radar backscatter data and integrates vegetation and climate information, such as tree cover, tree density, and background climate data, to enhance the accuracy of global AGC mapping. Our dataset estimates an average global above-ground carbon stock of 378 PgC, aligning with other global estimates. We observe a slight gross increase of 1.18 PgC in global vegetation above-ground biomass carbon stocks from 1993 to 2020, with relatively stable variation. This reflects a balance between above-ground biomass carbon gains and losses across different biomes. Temperate and boreal forests are the primary contributors to global vegetation above-ground biomass carbon gains from 1993 to 2020, with increases of 0.4 and 0.5 PgC, respectively. In contrast, gross above-ground biomass carbon losses are predominantly observed in global tropical forests (-10.7 PgC) and global shrublands (-1.0 PgC). This suggests non-forest vegetation may offset the large above-ground biomass losses in tropical forests. Notably, El Niño events in 2015/16 triggered significant pantropical AGC losses of approximately -2.86 PgC, and regions with reported tree mortality events (Hammond et al., 2022) exhibited local AGC density declines of -0.34 MgC/ha. This long-term, temporally continuous, and moderate-resolution dataset provides a valuable resource for understanding biomass carbon dynamics and integrating these processes into Earth System Models. The AGC dataset is openly accessible, alongside with this manuscript.

1 Introduction

Terrestrial ecosystem biomass plays a key role in the global carbon cycle (Friedlingstein et al., 2023) and is crucial for developing effective carbon emission mitigation strategies (Bonan, 2008). Above-ground biomass carbon (AGC), the most dominant and dynamic component of terrestrial ecosystems, accounts for approximately 30% of the total terrestrial carbon sink by sequestering and storing carbon in plant tissues (Beer et al., 2010). However, AGC can also contribute to the terrestrial carbon source, particularly in response to extreme events and disturbances such as drought, wildfires, deforestation, and changes in

https://doi.org/10.5194/essd-2025-330
Preprint. Discussion started: 24 July 2025

land use (Liu et al., 2011a; Williams et al., 2016; Dye et al., 2024). The trade-off of these two impacts on AGC in the context of increasing extreme events and disturbances determines the carbon dynamics and budgets for terrestrial ecosystems (Reichstein et al., 2013; Frank et al., 2015; Pugh et al., 2019). Therefore, long-term mapping and estimating AGC is essential to understand the carbon dynamics and fate of terrestrial ecosystems, reduce uncertainties in global carbon budget estimates, and formulate land-based climate mitigation policies.

Efforts to map and quantify AGC have primarily relied on field inventories (Pan et al., 2011, 2024), dynamic global vegetation models (DGVMs) (Friend et al., 2014; Ahlström et al., 2017; Yang et al., 2020a), and remote sensing techniques (Saatchi et al., 2011; Baccini et al., 2012; Liu et al., 2015; Xu et al., 2021; Yang et al., 2023). Inventories are a direct and precise way for estimating biomass carbon, supporting the quantification of, for example, global forest carbon changes (Pan et al., 2024) and carbon sources/sinks through Agriculture, Forestry and other Land Use in National Greenhouse Gas Inventories (Tubiello et al., 2021; Bastos et al., 2022). However, large-scale biomass change estimates based on inventory data have inherent limitations: measurements are based on small-scale plots with varying density depending on country/region, limited to forest ecosystems only and are typically carried out at 5-10 years intervals, methodological changes in inventories that may cause artifacts in long term changes, and most tropical forests / un-managed forests are not measured. DGVMs can estimate AGC globally at a coarse spatial resolution (e.g., 0.5°, (El-Masri et al., 2013)), but they often show inconsistencies with carbon flux from atmospheric inversions (Tagesson et al., 2020) due to incomplete representation of biogeochemical processes, disturbances and forest management (Pugh et al., 2019). Compared to these two approaches, remote-sensing has emerged as a promising way of quantifying forest biomass carbon in a spatially and temporally continuous manner and with global coverage. Currently, static AGC maps for specific years and dynamic continuous AGC maps have been produced using optical (Gibbs and Ruesch, 2008; Hu et al., 2016; Yang et al., 2020b), lidar (Saatchi et al., 2011; Baccini et al., 2012; Xu et al., 2021), radar (Besnard et al., 2021; Santoro et al., 2021), and passive microwave (Liu et al., 2015; Fan et al., 2019; Yang et al., 2023) techniques. Static AGC maps, generated at high spatial resolutions from 100 to 1000 meters, offer detailed spatial distribution insights and serve as baselines for future carbon stock change estimates. However, they mainly provide a snapshot of biomass at a single year, lacking information on temporal changes. This limitation makes it challenging to identify AGC temporal dynamics, despite AGC's large temporal variability. Dynamic continuous AGC maps offer opportunities to monitor AGC dynamics. For instance, pantropical or global dynamic continuous AGC maps (Liu et al., 2015; Fan et al., 2019; Besnard et al., 2021; Yang et al., 2023) with a spatial resolution of 25 km were produced using vegetation optical depth (VOD) around 10 years or radar satellite data from 1992-2018. These products have contributed to improve our understanding of biomass carbon dynamics, for example to map carbon losses and gains due to deforestation, forest degradation and management (Heinrich et al., 2021; Xu et al., 2021; Fawcett et al., 2023; Heinrich et al., 2023), quantify biomass responses to disturbances such as droughts or fires (Fan et al., 2023, 2024), evaluate reported sinks/sources by national greenhouse gas inventories (Fang et al., 2024; Lauerwald et al., 2024) and quantify drivers of trends in regional carbon budgets (Winkler et al., 2023). However, most current satellite biomass products either have limited long-term biomass records (for instance European Space Agency's Climate Change Initiative (CCI) data, 2010, 2017-2021 available) (Santoro and Cartus, 2023) or coarse spatial resolution of 25 km (Yang et al., 2023) which can lead to a loss of accuracy in predicting carbon dynamics due to averaging.

https://doi.org/10.5194/essd-2025-330
Preprint. Discussion started: 24 July 2025

AGC dynamic changes mainly result from three processes: physiological processes such as photosynthesis and growth, natural disturbances and recovery, and anthropogenic activities like land use changes (Houghton et al., 2009). These processes influence on AGC is usually slow-in and fast-out, and also legacy effects and slow recovery (Harris et al., 2016; Yang et al., 2020c). Large-scale and instantaneous impacts could be detected by the current short-term and coarse AGC dataset. However, evaluating the impacts on biomass carbon from slow-developing and small-scale processes such as biotic disturbances, tree mortality, or recovery dynamics requires high-resolution and long-term biomass data (McDowell et al., 2015). To circumvent these issues, space for time substitution based on high resolution biomass maps such as the ESA-CCI ones is often used to quantify AGC changes due to following disturbances (Xu et al., 2021; Yang et al., 2023; Feng et al., 2024). However, space for time substitution relies on the assumption that other environmental factors contributing to spatiotemporal variability in biomass can be ignored, which might not hold under the current pace and magnitude of global environmental change.

The recent long-term high-resolution radar backscatter data by Tao et al. (2023) provides a valuable opportunity to map biomass changes globally at moderate spatial resolution (8km) and over almost three decades. Based on this new dataset, we generate a new long-term and moderate-resolution global AGC dataset from 1992 to 2020 through a machine learning upscaling model trained on high-resolution AGC data from ESA CCI and including additional climatic and environmental predictors. We then quantify global and regional AGC stocks and sinks, and their spatial and temporal variability over the study period.

2 Materials and Methods

2.1 Data

2.1.1 Satellite radar backscatter data

In this study, we used the satellite radar backscatter dataset from Tao et al. (2023) to estimate AGC, based on merged signals from the C-band European Remote Sensing satellite (ESA)/ Advanced SCATterometer (ASCAT) and Ku-band Quick Scatterometer (QSCAT). This dataset provides long-term monthly satellite radar backscatter time series from 1992 to 2020 at a moderate resolution of approximately 8.9 km (compared to the commonly used 25 km resolution) and covering most global land areas. Initially, this radar backscatter dataset was re-gridded to a resolution of 8 km (~0.083 degrees).

Radar backscatter is considered a useful indicator for AGC, but it can also be influenced by variations in vegetation water content and surface water (Liu et al., 2011b; Konings et al., 2019; Wigneron et al., 2021). To reduce potential noise from short-term variations in vegetation water content, we applied a 12-month moving average on the radar backscatter time series. We then computed the mean radar signal for each pixel annually to create yearly radar backscatter data, thereby minimizing the influence of moisture. Pixels with outlier values identified via standard deviation were excluded from this study. We further excluded pixels where the areal fraction of regularly flooded wetlands or lakes exceeds 80%, based on the global wetland maps from Tootchi et al. (2019). Additionally, we removed pixels with peatland fractional coverage greater than 10%, using the global peatland map from Melton et al. (2022). As our study focuses on vegetation, we also masked out bare areas (total

https://doi.org/10.5194/essd-2025-330
Preprint. Discussion started: 24 July 2025

vegetative cover < 4 %) using CCI land cover map (Harper et al., 2023). We removed the radar backscatter data for 1992 due to large data gaps in that year.

2.1.2 Biomass reference data

Here we use the global above-ground biomass maps at 100m spatial resolution for the years 2017-2020 from the European Space Agency's Climate Change Initiative version 4 (Santoro and Cartus, 2023) as reference data. These datasets were aggregated from a resolution of 100 m to 8 km by averaging the values to match the resolution of the radar backscatter data. The same filtering method used to mask wetlands, peatlands, and bare areas in the radar backscatter data was also applied to this biomass reference data.

2.1.3 Climatic variables

The climate dataset, including monthly maximum temperature, minimum temperature and precipitation accumulation, was obtained from TerraClimate (https://www.climatologylab.org/terraclimate.html) with a spatial resolution of ~4km from 1991 to 2020 (Abatzoglou et al., 2018). To match the spatial resolution required for this study, these data were aggregated from 4 km to 8 km using mean values. The monthly mean temperature was calculated from the monthly maximum and minimum temperatures during 1991-2020. Subsequently, we calculated the mean annual temperature (MAT) and mean annual precipitation (MAP) for the period 1991-2020 to represent the background climate.

2.1.4 Land cover information

In this study, we aimed to map AGC map from radar backscatter data based on the relationships between AGC and radar backscatter. However, these relationships vary with environmental conditions and vegetation properties (Yu and Saatchi, 2016). To refine our AGC predictions, we incorporated additional information about tree cover and density, namely the global high-resolution (30m) tree cover map in 2000 based on global Landsat data by Hansen et al. (2013), and the global tree density map at the 1-km^2 spatial scale developed by upscaling 429775 ground-based tree density measurements with a predictive regression model by Crowther et al. (2015). To define the study biome, we integrated the global ecoregion map within 14 biomes (Olson et al., 2001) with the CCI land cover map to generate a globle land cover map (Harper et al., 2023) to 7 major biomes, including tropical American forest, tropical African forest, tropical Asian forest, temporate American forest, temporate Eurasian forest, boreal forest, and shrublands. All these maps were aggregated to 0.083 degree resolution by averaging, matching the resolution of the radar backscatter data to ensure spatial consistency across all datasets.

2.1.5 Tree mortality events

We evaluated whether our new AGC dataset is able to characterize temporal variability in biomass for reported tree mortality events in the recent decades. For this, we used the global tree mortality dataset based on forest inventory from the International Tree Mortality Network's Global Tree Mortality Database (http://tree-mortality.net/globaltreemortalitydatabase)

https://doi.org/10.5194/essd-2025-330
Preprint. Discussion started: 24 July 2025

120 covering drought-related tree mortality events from 1970 to 2020 (Hammond et al., 2022). In this study, we focused on tree mortality events reported between 1995 and 2018, excluding those from the first two and last two years to explore the footprint of tree mortality impacts on AGC. A total of 1186 tree mortality events were reported during this period.

2.2 Methods

2.2.1 Machine learning model

125 Here we trained random forest regression models to derive global models for AGB estimates based on the radar backscatter signal (Rad) and the referenced AGC maps from ESA-CCI for the period 2017-2020. Given that the relationships between AGC and the radar backscatter are likely to vary with background climate and vegetation properties, we additionally tested models that included tree cover (Tc), tree density (Td) and background climate (Clim, including MAT and MAP). In total, we tested eight different global-scale random forest models of above-ground biomass based on combinations of the radar 130 backscatter with these additional predictors (Table 1). We used leave-one-year-out cross-validation to train and test our global random forest models. This approach involved training the models on datasets from three years (sample numbers: 3587793) and testing them on a dataset from one year (sample numbers: 1195931). For model evaluation, we primarily computed the root mean square error (RMSE), the coefficient of determination (R^2) and Bayesian information criterion (BIC) for both training and testing samples in each cross-validation iteration across all random forest models. The mean R^2, RMSE, and BIC values 135 from all cross-validation iterations were computed for both training and testing data. The best model was selected according to the smallest BIC. The model uncertainty (Unc) between the different models builded in each cross-validation iteration was also calculated using the equation (1).

$$Unc = std(\sum(obs_i\text{-}pred_i) / N_i) \quad (1)$$

where, Unc is the model uncertainty. i represents each model developed in each cross-validation iteration, obs_i and $pred_i$ are 140 the observed and predicted AGC values for model i, N_i is the number of observations for model i, std is the standard deviation across the mean errors of all models.

2.2.2 Analysis of spatial and temporal dynamics in AGC

We further applied this best random forest model to predict the global AGC changes for the study period from 1993 to 2020 based on the satellite radar backscatter data. The coefficient of variation (CV) of AGC carbon density was calculated to assess 145 the variability in carbon density estimates. The coefficient of variation (CV) is calculated as the ratio of the standard deviation (σ) to the mean (μ), expressed as a percentage:

$$CV = \left(\frac{\sigma}{\mu}\right) \times 100$$

(2) Where σ is standard deviation of AGC carbon density, μ is mean AGC carbon density.

The carbon stock for each pixel was derived by multiplying the carbon density by the pixel area. To evaluate changes 150 in carbon storage over time, we computed the net carbon sink for each biome by analyzing the differences in carbon stock

https://doi.org/10.5194/essd-2025-330
Preprint. Discussion started: 24 July 2025

between two time points (equation (3)). Given the slow rate of net carbon sink changes, we calculated the decadal carbon sink for three distinct periods: 1993–1999, 2000–2009, and 2010–2019.

C_{sink} (t) = C_{stock} (t) - C_{stock} (t-1) (3)

where C_{sink} (t) represents the carbon sink for the year (t). C_{stock} (t) and C_{stock} (t-1) are the carbon stocks at year (t) and (t-1), respectively.

3 Results

3.1 Above-ground biomass model performance

The performance of the eight AGC models varies significantly based on the predictors used and their ability to generalize to unseen data (Table 1). The random forest regression model based solely on radar backscatter (Rad model) shows a high training R^2 (0.894) but a very low R^2 in testing samples (0.228), indicating severe overfitting and poor generalization, as evidenced by the large RMSE in testing set (66.5 MgC/ha). Adding vegatation structure information either Tc (Rad_Tc model) or Td (Rad_Td model) increases R^2 in the testing samples substantially (up to 0.904 and 0.812 respectively) while reducing RMSE and BIC. The Rad_Clim model including background climate achieves a high training R^2 (0.987) and testing R^2 (0.911), with low RMSE in training (8.6 MgC/ha) and testing samples (22.5 MgC/ha), which shows it maintains good predictive accuracy on the test set. The inclusion of vegetation structure and background climate as a predictor significantly improves the model's performance compared to using Rad alone, highlighting the importance of incorporating vegetation structure properties and background climate for accurate predictions.

Given that the environmental predictors are expected to be partly co-correlated with each other (e.g., tree density and background MAT and MAP), we further evaluated whether their joint consideration improves model performance. We tested combinations of radar backscatter with two environmental predictors and, finally, a combination of all four predictor groups (n predictors = 5). For models with three (except Rad_Clim model) or four predictor groups, we find significant improvements in both training and test performance. In the training data, these models achieve high R^2 values, ranging from 0.995 to 0.998, indicating an excellent fit to the observed data. Similarly, in the test data, the R^2 values improve substantially, ranging from 0.972 to 0.985, demonstrating strong generalization capabilities. Additionally, the RMSE for the test data is reduced by about half compared to models with only two predictor groups, with test RMSE values falling between 7.5 and 12.7 MgC/ha, compared to 23.4–32.8 MgC/ha for models with two predictors.

The Rad_Tc_Td_Clim model, integrating tree cover, tree density, and background climate with radar backscatter, is found to be the most effective in predicting above-ground biomass, with with the highest test R^2 (0.990), lowest test RMSE (7.5 MgC/ha), and lowest test BIC (4794276), indicating it balances complexity and accuracy effectively. Based on these results, we selected Rad_Tc_Td_Clim model as the final model for generating AGC predictions from 1993 to 2020.

https://doi.org/10.5194/essd-2025-330
Preprint. Discussion started: 24 July 2025

Open Access Earth System Science Data Discussions

Table 1. Model predictors and model performance metrics: R^2, RMSE (MgC/ha), and BIC in training and testing dataset (mean performance across cross-validation train and test sets) for random forest regression models of above-ground biomass carbon. The datasets consisted of 3,587,793 training samples and 1,195,931 testing samples.

Random Forest Model	Predictor	R^2_train	R^2_test	RMSE_train	RMSE_test	BIC_train	BIC_test
Rad	Rad	0.894	0.228	24.6	66.5	22992531	10039390
Rad_Tc	Rad, Tc	0.985	0.904	9.3	23.4	16022428	7544703
Rad_Td	Rad, Td	0.972	0.812	12.8	32.8	18268398	8349254
Rad_Clim	Rad, MAT, MAP	0.987	0.911	8.6	22.5	15465268	7446607
Rad_Tc_Td	Rad, Tc, Td	0.996	0.976	4.6	11.6	10871888	5851018
Rad_Tc_Clim	Rad, Tc, MAT, MAP	0.998	0.985	3.4	9.3	8776514	5323870
Rad_Td_Clim	Rad, Td, MAT, MAP	0.995	0.972	5.2	12.7	11875255	6072943
Rad_Tc_Td_Clim	Rad, Tc, Td, MAT, MAP	**0.998**	**0.990**	**3.0**	**7.5**	**7841172**	**4794276**

3.2 Spatial pattern of above-ground biomass

Based on our new radar-based models, we estimate a mean above-ground biomass carbon density for global vegetation of 55.0 MgC/ha during 1993 to 2020 (excluding 1997 due to the low data quality), with large regional variations (Figure 1 A): tropical forests show high AGC densities (215.4 MgC / ha), followed by mid-latitude forest (54.9–93.2 MgC/ha). Interannual variability of AGC is high in arid and semi-arid regions, and low in humid areas with high biomass densities (Figure 1 B). The global mean above-ground biomass carbon stock is estimated at 378.4 (±1.7) PgC during 1993 to 2020 (excluding 1997). Forest ecosystems hold 61% of the AGC carbon stocks (230.0 PgC aggregated), with the large majority (181.5 PgC, i.e. 79% of forest AGC) being located in the tropical regions: 109.4 PgC, 42.0 PgC and 30.0 PgC for tropical forests in South America, Africa and Asia, respectively. In total, temperate forests in the American and Eurasian regions store 30.0 PgC in above-ground biomass, and boreal forests 19.5 PgC. In non-forest ecosystems, shrublands correspond to the AGC pool of 5.6 PgC.

3.3 Temporal changes of above-ground biomass

3.3.1 Trends in AGC

Our dataset shows a widespread increase globally in carbon density from 1993 to 2020 (Figure 2A), with an average growth rate of 0.003 MgC/ha/year but large regional variations. Approximately 48% of the vegetated land area exhibits increasing trends at an average rate of 0.22 MgC/ha/year, primarily located in Southern Africa, Central Europe, the northeastern part of North America, and Southern China. Conversely, we find declining trends in Central and South America, Northeastern Europe, and Southeastern Russia, corresponding to 51% of the vegetated area, and an average rate of -0.21 MgC/ha/year. Given these contrasting trends, the global mean aboveground biomass carbon is mostly stable over 1993–2020, with a mean value of 378 PgC (Figure 2B). This stability is maintained by a decadal net carbon sink fluctuating between -0.19 and +0.58 PgC/year (Figure 2B, grey bars). For areas with positive AGC trends (Figure 2A), we estimate a gross AGC gain of ca. 19 PgC from

https://doi.org/10.5194/essd-2025-330
Preprint. Discussion started: 24 July 2025

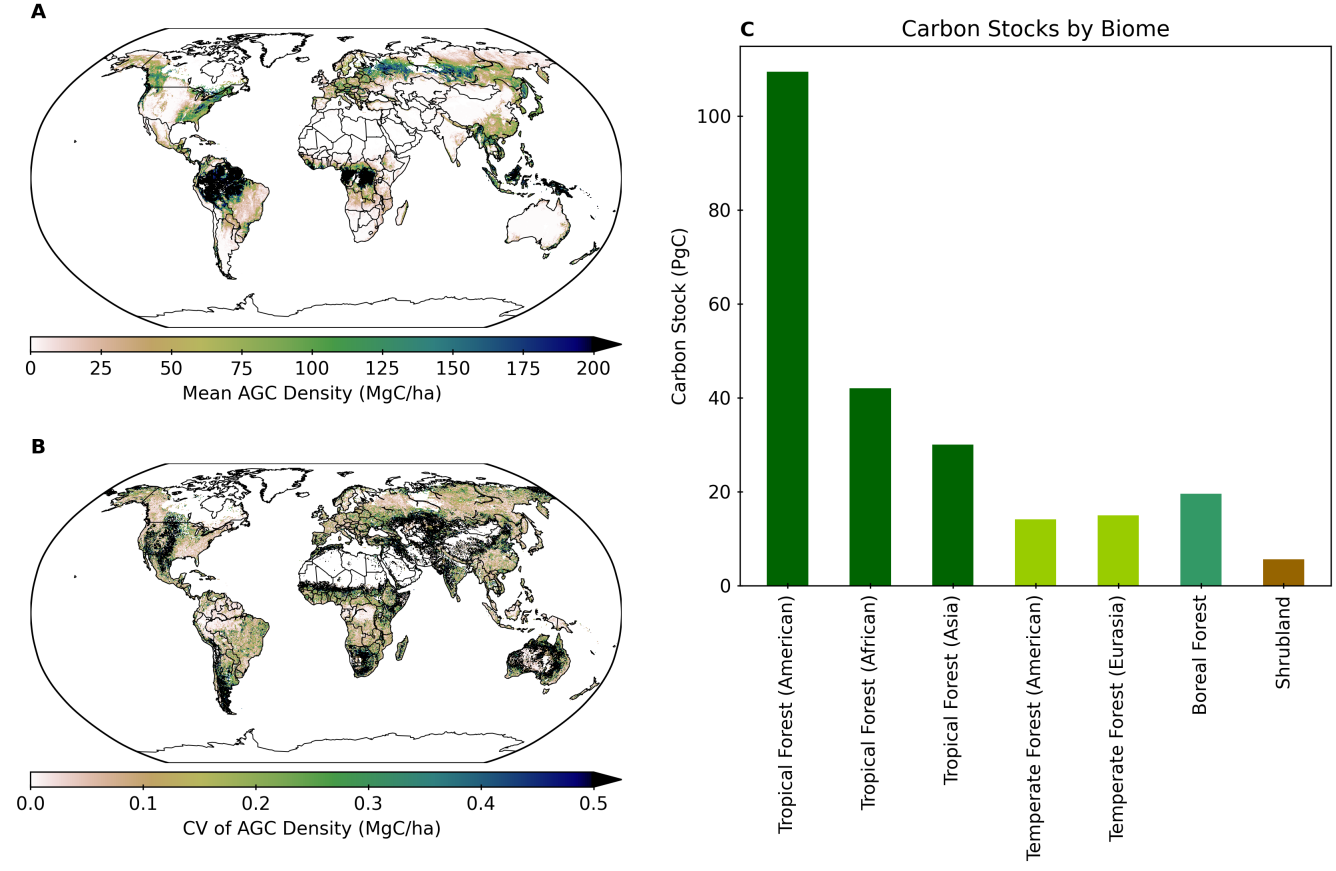

Figure 1. Mean above-ground biomass carbon (AGC) density and stocks from 1993 to 2020 (excluding 1997 due to low data quality). (A) Spatial distribution of mean global above-ground carbon density and (B) corresponding CV (coefficient of variation). (C) Above ground biomass carbon stocks aggregated for global biomes.

1993 to 2020, with a mean carbon gain rate of 0.73 PgC/year (Figure 2C). These carbon gains are supported by the strong increasing decadal net carbon sink rate, from a mean net carbon sink in aboveground biomass of about 0.63 PgC/year in 1990s to 0.74 PgC/year in 2010s (Figure 2C). In contrast, regions with declining AGC trends (Figure 2D) experienced a gross loss of 18 PgC (rate: -0.74 PgC/year), driven by persistent carbon emissions (e.g., -0.88 PgC/year in 2000s). These two contrasting trends result in a net sink in aboveground biomass of 0.38 PgC/year (Figure 2B).

AGC carbon stock trends also differ widely across biomes (Figure 3). Forests worldwide contributed to a gross carbon stock loss of AGC of -9.9 PgC (2020 minus 1993) in the period 1993–2020, while shrublands registered a net loss of -1.0 PgC corresponding to mean sink in aboveground biomass of -0.04 PgC/year, respectively. The AGC sink in global forests in 1993–2020 was predominantly located in temperate forests, with a net gain of 0.36 PgC at a net rate of 0.01 PgC/year, while tropical forests offset these gains through a net loss of -10.7 PgC and a mean sink of -0.4 PgC/year. Temperate forests show

https://doi.org/10.5194/essd-2025-330
Preprint. Discussion started: 24 July 2025

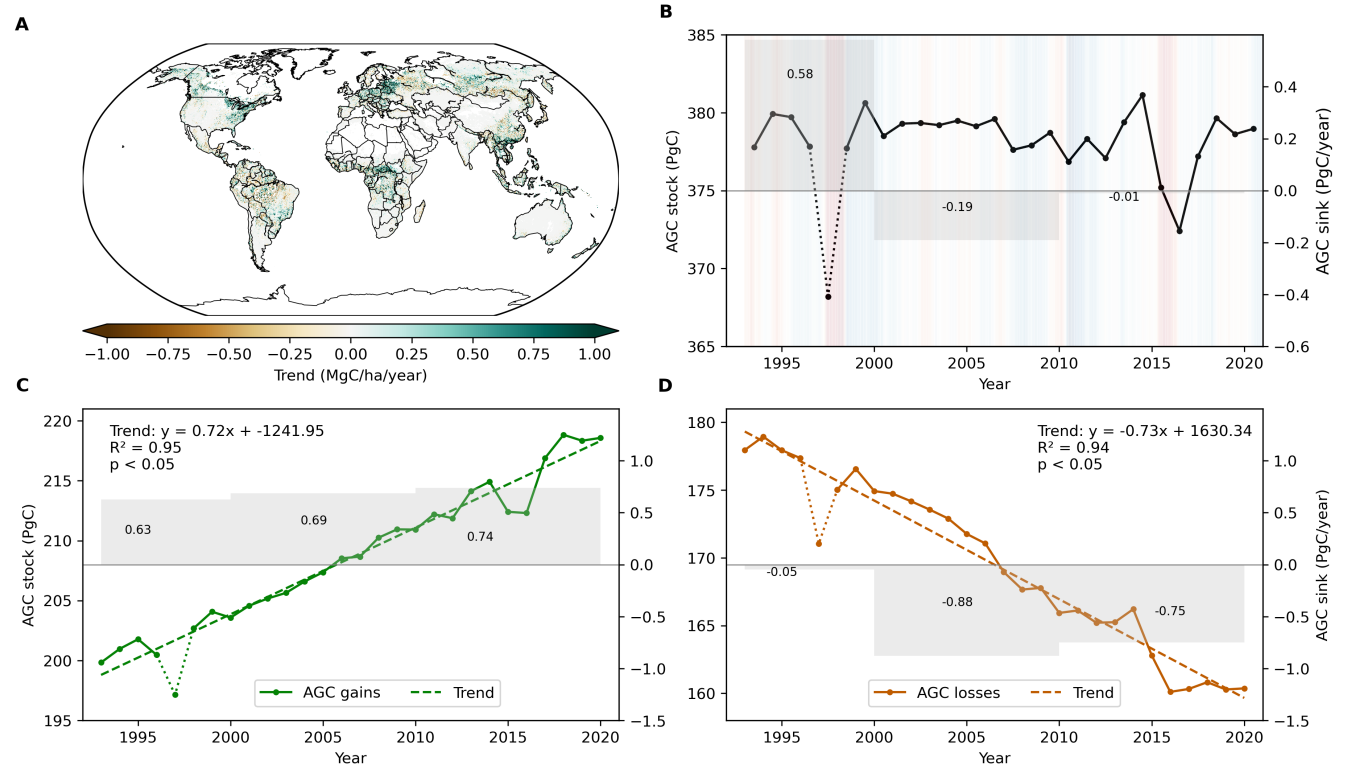

Figure 2. Trend in global above-ground biomass during 1993 to 2020. (A) Global vegetation above-ground carbon density trend map. (B) Changes in global annual vegetation above-ground carbon stock (left y-axis) and decadal mean carbon sink (grey bar, right y-axis). The shades in the background show the ENSO states (red – El Nino and blue – La Nina). (C) Changes in annual above-ground carbon stock (left y-axis) and decadal mean carbon sink (grey bar, right y-axis) in regions with increasing trends of above-ground biomass. (D) Changes in annual above-ground carbon stock (left y-axis) and decadal mean carbon sink (grey bar, right y-axis) in regions with decreasing trends of above-ground biomass. Carbon sink values are displayed adjacent to the grey bars. Dashed lines in (C) and (D) represent trend lines for annual carbon stock changes, with trend equations, R^2, and p-values provided. Dotted lines in 1997 highlight estimates that may be affected by unreliable data quality.

https://doi.org/10.5194/essd-2025-330
Preprint. Discussion started: 24 July 2025

significant (P < 0.05) increasing trends in AGC, with a carbon gain rate of 0.01 PgC/year in both American and Eurasian forests (Figure 3 E-G). In Eurasian forests, AGC increased by approximately 0.4 PgC from 1993 to 2020, with 46.0% of these forests showing a net gain of 1.5 PgC at a rate of 0.06 PgC/year. Correspondingly, the decadal net carbon sink in Eurasian temperate forests increased from -0.07 PgC/year in the 1990s to 0.04 PgC/year in the 2010s. Boreal forests also contribute the most to carbon sink from 1993 to 2014, with a gain of approximately 1.6 PgC at a net rate of 0.05 PgC/year. However, from 2015, boreal forests experienced significant variability, with a sustained carbon loss about -0.01 PgC. AGC losses in tropical forests from 1993 to 2020 are primarily attributed to a substantial decrease in AGC in tropical America, with a loss of -10.0 PgC at a significant (P < 0.05) average rate of -0.39 PgC/year over the whole period, while tropical African and Asian forests show only slightly declining AGC -0.6 PgC and -0.1 PgC respectively, with a mean aboveground biomass loss rate of -0.02 PgC/year and 0.0 PgC/year, respectively.

3.3.2 Interannual variability

In addition to the long-term trends, we evaluate interannual variability in AGC stocks. Globally, notable declines in AGC occurred in 1997 and 2015/16 (Figure 2 B), coinciding with two strong El Niño events. Due to the possible data quality problem in 1997, here we only focus on 2015/2016 El Niño event. In 2015/16, decline in global mean AGC compared with 2014 is around -7.3 PgC. Tropical forests contribute 40% declines about -2.9 PgC on the globle declines (Figure 3). The declines of carbon stock were smaller in tropical African and Asian forests compared to American forests (-0.4, -0.6 and -1.9 PgC, respectively). Following the El Niño events, tropical African and Asian forests recovered quickly, surpassing pre-El Niño AGC levels by 2017 compared to 2014. In contrast, tropical American forests continued to decline despite partial recovery, consistent with the strong long-term decline in AGC.

Shrublands also show declines in AGC during the two El Niño events, though smaller in magnitude. In contrast, the La Niña event in 2011 result in small AGC gains globally (Figure 2 B), primarily in boreal forests and shrublands rather than other forest regions (Figure 3). Beyond ENSO variability, our long-term AGC dataset also find the extreme events impact on AGC. For example, boreal forests experienced a significant decline in 2010, likely related to drought events.

3.4 Tree mortality and AGB carbon changes

Finally, we evaluate whether our long-term and moderate resolution dataset allows to detect impacts of tree mortality on AGC for events reported between 1995 and 2018 (Figure 4). Tree mortality events are associated with AGC losses, with a median carbon density anomaly values (relative to the reference period of 1993–2020) of -0.35 MgC/ha, and the 25th and 75th percentiles ranging from -2.0 to 0.03 during the reported mortality year. Our dataset shows, however, a multi-year temporal pattern, with predominantly positive anomalies two years prior to the mortality event (0.22, -0.34–1.6 MgC/ha) and a slow decline (-0.11, -0.64–0.27 MgC/ha) already in the year prior to the mortality event. Following tree mortality events, AGC density shows partial recovery with median AGC of -0.044 MgC/ha and -0.037 MgC/ha in the first two recovery years, but with assymetric spatial distribution in recovery dynamics: in the first year, the 75% percentile of AGC anomaly still corresponds to low biomass density values (0.12 MgC/year), while in the second year the value increases rapidly to 1.6. However, half of

https://doi.org/10.5194/essd-2025-330
Preprint. Discussion started: 24 July 2025

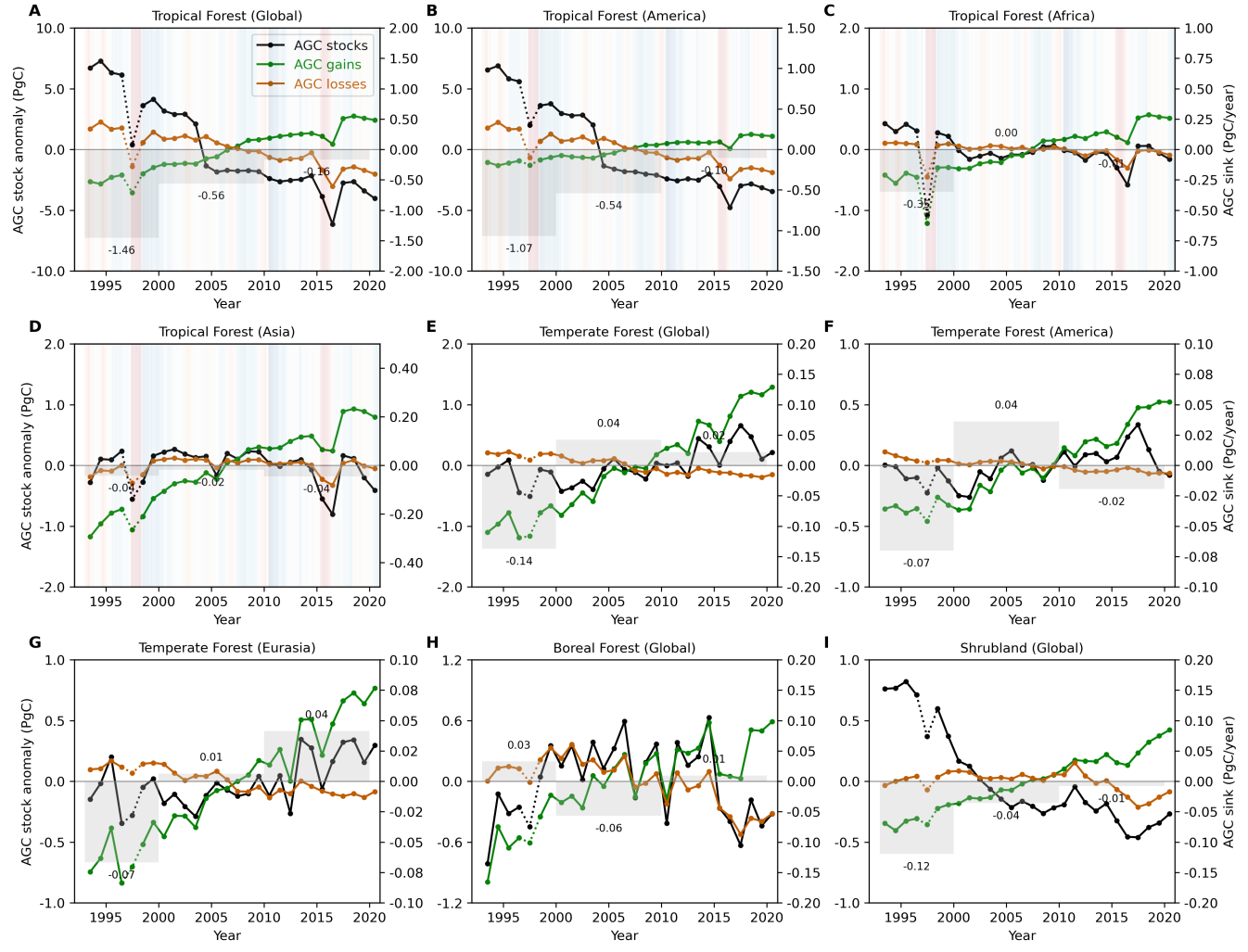

Figure 3. Temporal patterns of annual anomalies in above-ground carbon stocks (black line), carbon gains (green line, representing regions with increasing above-ground biomass trends), carbon losses (brown line, representing regions with decreasing above-ground biomass trends), and decadal mean carbon sink (grey bar) for each biome. Carbon sink values are displayed adjacent to the grey bars. The shades in the background of pannel A-D show the ENSO states (red – El Nino and blue – La Nina). Dotted lines in 1997 highlight estimates that may be affected by unreliable data quality.

https://doi.org/10.5194/essd-2025-330
Preprint. Discussion started: 24 July 2025

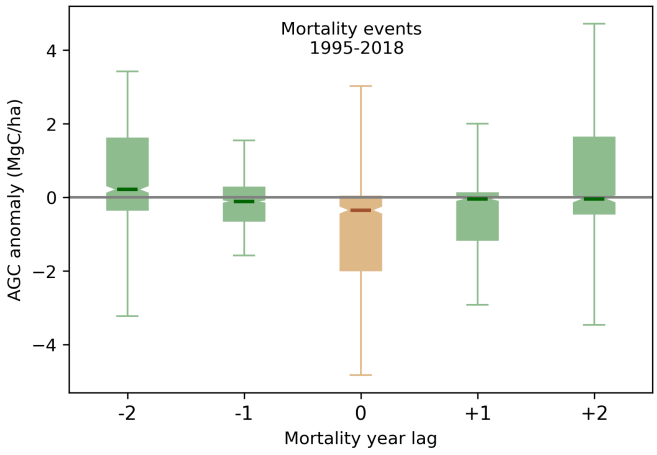

Figure 4. Mortality AGC fingerprint (from two years before to two years after tree mortality) for global tree mortality events from 1995 to 2018

the pixels show much slower recovery, with the 25% percentile corresponding to -1.16 MgC/ha and -0.44 MgC/ha in the first and second year following mortality, respectively. For most events, the forests did not fully recover to the AGC density levels prior to the mortality events.

4 Discussion

In our study, we generated a new long-term, high-resolution above-ground biomass dataset using satellite radar backscatter data. This dataset provides continuous biomass estimations over approximately 30 years from 1993 to 2020, making it the longest continuous biomass dataset currently available. Furthermore, our dataset has a fine resolution of 8 km, significantly higher than the 25 km resolution of other biomass products based on X-band or L-band vegetation optical depth (L-VOD) estimates (Liu et al., 2015; Fan et al., 2019; Yang et al., 2023). These biomass products firstly compute the VOD based on the microwave radiometer signals, and then fit the empirical relationships between VOD and AGC from satellite-based reference maps at continental scale (Fan et al., 2019; Yang et al., 2023). Here, we developed one machine learning global model to predict AGC for all vegetation types and landscapes. Unlike empirical parametric models (e.g., Liu et al., 2015; Rodríguez-Fernández et al., 2018; Fan et al., 2019; Yang et al., 2023), we combined radar backscatter information with additional environmental predictors, namely, tree cover, tree density, and background climate in a random forest regression model. Random forest regression allows to derive estimates of AGC that consider regional differences in the relationship between the radar back-scatter and AGC due to background climate (e.g. semi-arid vs. tropical regions) and to account for co-variation in the environmental predictors considered (e.g., tree density and background climate). Our model, driven by these factors, outperforms simple models based solely on radar backscatter (Table 1), emphasizing the importance of considering climate and vegetation properties in AGC estimations. Although incorporating these additional predictors increases model complexity, it effectively balances model

https://doi.org/10.5194/essd-2025-330
Preprint. Discussion started: 24 July 2025

complexity and accuracy, which is evidenced by achieving the highest R^2 and the lowest RMSE and BIC values among all random forest regression models developed in this study (Table 1).

4.1 Comparison with other global above-ground biomass maps

4.1.1 Comparison in the spatial pattern of global above-ground biomass

Overall, our estimates of global mean above-ground biomass carbon stock of 378 PgC for the period 1993–2020, align well with other global AGC datasets (e.g., Liu et al., 2015; Xu et al., 2021; Santoro and Cartus, 2023; Yang et al., 2023; Pan et al., 2024) that range from 358–380 PgC, excepting that by Besnard et al. (2021), which estimates considerably lower global AGC (248 PgC) than all other datasets (Table 2). Compared for the same reference period and same spatial coverage, our estimates are slightly higher than those from Xu et al. (2021), and lower than those from SMOS L-VOD (Yang et al., 2023). Compared to inventory estimates Pan et al. (2013), we focus on the forests to to maintain consistency with their methodology. While our AGC stock estimates are very slightly lower or larger, they remain broadly consistent with their estimations. The absolute difference between this study and other AGC datasets, excluding ESA CCI used to train our model, ranges from -31.2 PgC to 11.2 PgC (i.e., roughly 3–8%). The underestimation compared to SMOS L-VOD from Yang et al. (2023) might be because our AGC dataset is based on C-band radar backscatter, which can not capture under-ground biomass as well as L-band. A potential reason for overestimation of global carbon stocks might relate to the extent of vegetated area considered. In our study, we focus on the global vegetation area, excluding wetland, barren area, regions with peatlands covering more than 10%, grasslands, and croplands. While other studies are focused on woody vegetation (Xu et al., 2021), this excluding of AGC in non-woody or non-forest area makes our estimate higher than that reported in those studies.

The mean global spatial pattern of above-ground carbon density derived in this study was compared with existing AGC products (Figure S**??**). Here we focused on four AGC datasets overlapping with the 2010–2019 period: 1) ESA-CCI, 2)Besnard et al. (2021), 3) Xu et al. (2021), 4) SMOS, estimates from Yang et al. (2023). Our results indicate that tropical forests exhibit the highest AGC density globally, followed by mid-latitude forests and non-forest ecosystems (Figure 1), a spatial pattern consistent across all four benchmark products (Figure S**??**). However, while the magnitude of AGC density in our map aligns closely with ESA-CCI and SMOS estimates, it is systematically higher than those reported by Besnard et al. (2021) and Xu et al. (2021). These differences might be cause by the different methods (e.g. statistical and data-driven), different satellite data and different vegetated areas used for deriving AGC density dataset.

4.1.2 Comparison in the temporal pattern of global above-ground biomass

Our analysis of above-ground biomass carbon stock changes between 1993 and 2020 reveals a slight increase along with relatively stable global carbon stock dynamics (Figure 2). Globally, we observed two contrasting trends (carbon gains and carbon losses) during 1993–2020, leading to a small net sink in above-ground biomass globally. This suggests that carbon gains—likely driven by forest regrowth due to longer growing season (Piao et al., 2007) and CO_2 fertilization (Walker et al., 2021) slightly outweighed the negative effects of carbon losses from climatic extremes (Yang et al., 2018), natural disturbances

https://doi.org/10.5194/essd-2025-330
Preprint. Discussion started: 24 July 2025

Open Access Earth System Science Data Discussions

Table 2. Comparison of global mean above-ground biomass carbon stocks between our product and other existing products. Note: The global mean above-ground biomass carbon stock for products marked with * is calculated based on the overlapping area between those products and our study area. Values for other products are taken directly from their respective publications.

Product	Period	Global (PgC)	This study (PgC)	Difference (PgC)
ESA-CCI (*)	2017	379.0	377.0	-1.9
	2018	378.8	379.5	0.6
	2019	378.5	378.4	-0.1
	2020	378.4	378.8	0.4
	2017-2020	378.7	378.4	-0.3
Xu et al., 2021 (*)	2000-2019	368.7	378.2	9.5
Besnard et al., 2021 (*)	1993-2019	248.0	378.1	130.1
Yang et al., 2023 (*)	2010-2020	358.4	327.2	-31.2
Liu et al., 2015	1998-2002	362.0	373.2	11.2
Pan et al., 2024	1990	379.7	371.4	-8.3
	2000	371.3	372.7	-1.4
	2010	374.1	371.4	-0.1
	2020	371.5	373.6	2.1

(Harris et al., 2016) and land-use changes (Winkler et al., 2023) during the study period. This finding aligns with recent field inventory-based studies, such as Pan et al. (2024), which report consistent carbon sinks across global forest ecosystems over the past 30 years. Furthermore, during the recent decade (2010–2019), the global AGC stock increased about 1.4PgC, with a mean net carbon sink of 0.19 PgC/year. This is consistent with another study reporting an increase in gross total living biomass carbon stock at a rate of 0.5 PgC/year (Yang et al., 2023). The difference in the estimated carbon stock increase rates between our study and others can be attributed to the scope of carbon stocks analyzed: our study focuses only on above-ground biomass carbon, while Yang et al. (2023) includes total living biomass carbon (which encompasses both above- and below-ground biomass). This distinction might explain the different variation rates in carbon stock trends.

The primary contributors to the global carbon gain during 1993–2020, as identified in our study, are temperate and boreal forests. Both American and Eurasian temperate forests exhibit significant increases in AGC stocks (Figure 3), with a growth rate of 0.01 PgC/year over the nearly three-decade study period. However, the temporal patterns of AGC gains differ between these two regions. In American temperate forests, AGC gains were primarily observed during the 2000s, followed by a stabilization and even carbon losses in recent years (around 2017). These recent carbon losses are likely attributable to recent disturbance events such as drought, insect outbreaks and wildfires (Harris et al., 2016; Fettig et al., 2022). In contrast, Eurasian temperate forests exhibited a progressively increasing net carbon sink, rising from 0.01 PgC/year in the 2000s to 0.04 PgC/year in the 2010s. These increase in AGC is supported by forest area expansion and improved forest management, longer growing seasons, CO_2 fertilization (Myneni et al., 2001; Erb et al., 2018; Etzold et al., 2020; Ameray et al., 2021; Yao et al., 2024).

https://doi.org/10.5194/essd-2025-330
Preprint. Discussion started: 24 July 2025

Boreal forests, on the other hand, gained carbon at a rate of 0.054 PgC/year from 1993 to 2014 but began losing carbon after 2015. These losses are likely due to their high sensitivity to climate variability (Eckdahl et al., 2022), increasing fire and logging disturbances (Mack et al., 2021; Wang et al., 2021; Shvetsov et al., 2021) and recent extreme events that resulted in AGC losses (Kwon et al., 2021). Despite these recent losses, the net carbon sink of 0.02 PgC/year—resulting from gains over the previous two decades and losses in recent years—indicates that boreal forests remain a net contributor to carbon gain, consistent with other studies (Xu et al., 2021; Yang et al., 2023; Pan et al., 2024).

Tropical forests, in contrast, are the primary contributors to global carbon losses. Among these, tropical American forests are the largest source of carbon loss. They exhibit a significant and persistent decline in AGC from 1993 to 2020, consistent with reports of reduced carbon sink capacity in Amazonian forests (Brienen et al., 2015; Baccini et al., 2017; Hubau et al., 2020). This decline is driven by deforestation, forest degradation, Amazon droughts, tree mortality, and slowing tree growth rates (Phillips et al., 2009; Lewis et al., 2011; Hubau et al., 2020; Gatti et al., 2021; Qin et al., 2021), as evidenced by negative AGC trends in the arc of deforestation (Figure 2). These findings align with recent reports indicating that tropical American forests are losing substantial carbon in a changing climate (Fawcett et al., 2023; Uribe et al., 2023; Pan et al., 2024). Tropical African and Asian forests also show slight, though not statistically significant ($P > 0.05$), decreases in AGC over the three-decade period. These losses are consistent with observed carbon declines due to land-use changes, such as the conversion of forests to agricultural land (Tyukavina et al., 2018; Feng et al., 2022), including the expansion of oil palm plantations in Southeast Asia (Vijay et al., 2016). In addition to tropical forests, our study identifies other non-forest ecosystems as contributors to carbon losses, particularly shrublands. Shrubland ecosystems have experienced significant and continuous declines in carbon stocks at a rate of -0.04 PgC/year over the study period. These losses may be attributed to grass invasions (Bradley et al., 2006). While shrublands contribute less to carbon loss than tropical American forests, their impact is greater than that of tropical African and Asian forests. This highlights the importance of understanding carbon dynamics in shrublands, given their relatively large contribution to carbon changes.

The impact of ENSO events on the dynamics and recovery of Aboveground Carbon (AGC) stocks is evident in our study. The 2015–16 El Niño caused substantial AGC losses of -2.86 PgC in tropical forests, consistent with documented declines from Bastos et al. (2018); Fan et al. (2019); Wigneron et al. (2020). Our findings on carbon loss magnitude from 2014 to 2016 align well with the reported loss of -1.63 PgC by Wigneron et al. (2020). Post-El Niño recovery processes also varied by continent. In tropical American forests, AGC stocks did not recover to pre-El Niño levels following either the 1997 or 2015–16 events. In contrast, tropical African and Asian forests exhibited faster recovery, returning to pre-El Niño AGC levels within a year. On a pantropical scale, AGC did not fully recover from these strong El Niño events, consistent with the findings of Wigneron et al. (2020).

Additionally, our study find the possible impact of other extreme events on AGC dynamics. For instance, a significant decline in AGC in boreal forests was observed in 2010 (Figure 3), likely due to drought-induced tree mortality (Peng et al., 2011). Similarly, the 2003 European heatwave (García-Herrera et al., 2010) led to AGC decreases in temperate Eurasian forests. Furthermore, the 2005 mega-drought in the Amazon (Marengo et al., 2008) resulted in a slight decline in AGC, with continued

https://doi.org/10.5194/essd-2025-330
Preprint. Discussion started: 24 July 2025

decreases potentially linked to the legacy effects of drought (Yang et al., 2018). These findings underscore the possibility of our new dataset to identify the extreme events impacts on carbon dynamics.

4.2 Uncertainty and limitation of our global above-ground biomass dataset

Our global above-ground biomass estimates are derived from the random forest regression models using radar scatter data, along with additional climate and forest structure predictors. While the models exhibit generally low mean uncertainty in global vegetation AGC predictions (Figure 5), indicating stable predictions across models trained in each cross-validation, regional variations exist. Higher uncertainties are observed in western and central Russian boreal forests, southeastern Asian tropical forests, and parts of tropical Africa and South America. Despite these localized uncertainties, the absolute AGC in these regions remains high, resulting in relatively low proportional uncertainty. One key source of uncertainty stems from the random forest regression models themselves. We employed a leave-one-year cross-validation approach to ensure robust wall-to-wall AGB estimation using radar scatter data. While this method enhances model generalizability, it does not fully eliminate uncertainties tied to regional variability in forest structure or environmental conditions.

Additionally, our global AGC stock in 1997 (Figure 2B) shows a sharp decline followed by rapid recovery in 1998, particularly in tropical African forests (Figure 3).). The substantial decline in AGC in 1997 may be attributed to the combined effects of three factors. First, the major El Niño event in 1997 affected plant growth, reducing carbon uptake and leading to a decrease in carbon stock. Second, the original satellite radar backscatter data contains sensor-related anomalies (Lecomte and Wagner, 1998). Third, anomalous radar signals in 1997 may reflect non-vegetation features, such as flooding, waterlogged land, or soil background effects, where surface water could act as a mirror and distort vegetation returns. Consequently, the 1997 data should be treated with caution, particularly in Africa.

Furthermore, our dataset is based on C-band satellite data, which is widely used for vegetation dynamics and biomass mapping (Besnard et al., 2021; Santoro et al., 2021). C-band satellite data, operating higher frequncies, tends to agree more closely with the dynamics in upper canopy. This characteristic may lead to the omission of lower canopy biomass, potentially resulting in an underestimation of the total biomass.

4.3 Advantages of our global dynamical above-ground biomass dataset

Our new above-ground biomass dataset offers primary advantages for tracking global biomass carbon changes and understanding key processes in biomass carbon dynamics, owing to its extended temporal coverage and fine spatial resolution. Traditional approaches in biomass studies, such as space-for-time substitution, have been widely used to assess disturbance impacts and recovery dynamics (Pickett, 1989). However, this method assumes that spatial differences directly correspond to temporal changes, which may not hold true due to variations in environmental conditions (e.g., soil type, climate) and disturbance regimes. These limitations hinder the accurate estimation of biomass carbon dynamics. In contrast, our dataset is based on real temporal changes in vegetation, providing a more accurate representation of temporal AGC dynamics compared to space-for-time substitution methods.

https://doi.org/10.5194/essd-2025-330
Preprint. Discussion started: 24 July 2025

Open Access Earth System Science Data Discussions

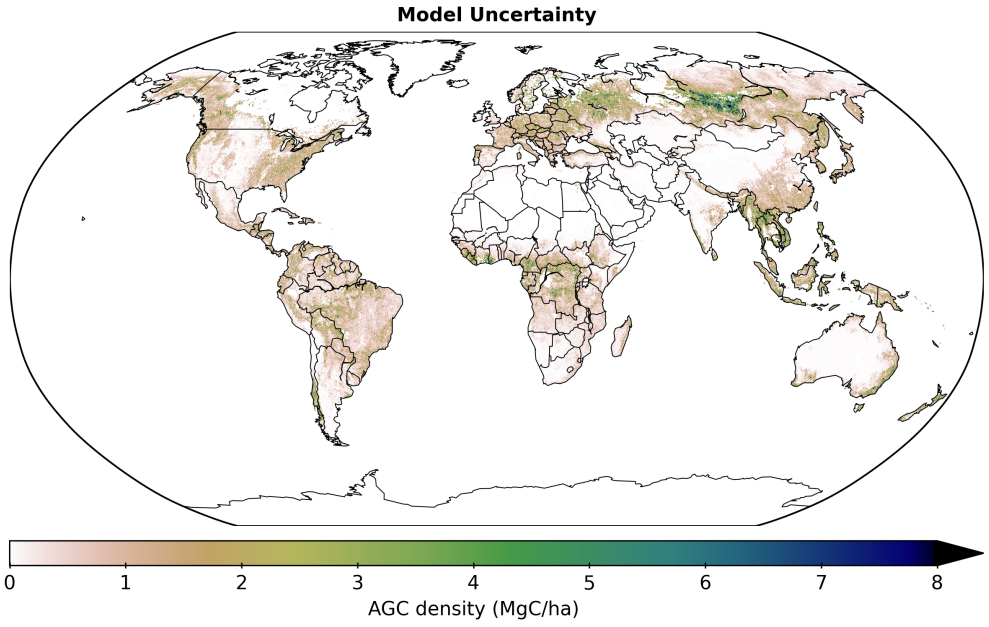

Figure 5. Model uncertainty for predicting above-ground biomass

Moreover, our long-term data can help unravel the complex impacts of climate change and disturbances on carbon dynamics. Climate change, along with increased ecosystem disturbances, is expected to produce more intricate carbon dynamics, particularly at regional and local scales (Franklin et al., 2016; Dye et al., 2024). For example, increasing droughts not only directly affect but also legacy effects on ecosystem carbon changes (Fleta-Soriano and Munné-Bosch, 2016; Kannenberg et al., 2020; Xu et al., 2021). Droughts can also trigger further disturbances, such as fires and insect outbreaks, thereby compounding stress on vegetation which lead to more tree mortality (Allen et al., 2010; Seidl et al., 2011; Anderegg et al., 2015; Burton et al., 2020). An increase in drought-induced tree mortality has been reported (Hammond et al., 2022), but remains challenging to detect in remote-sensing observations and to simulate in models (Hartmann et al., 2022). Additionally, human activities such as land-use change and management (Houghton, 2003; Lai et al., 2016) further complicate carbon dynamics. A major limitation in understanding of biomass changes in response to these extremes and disturbances is the fact that AGC datasets tend to be short-term or discrete, while understanding biomass losses from extremes, forest degradation and tree mortality, as well as recovery dynamics, require spatially and temporally continuous long-term datasets (Bustamante et al., 2016; Fu et al., 2017; Matricardi et al., 2020; Hartmann et al., 2022). Moreover, the disturbances often occuring at small spatial scales (25-100 m), require a pixel size close to the disturbance size (Houghton et al., 2009). our dataset, while relatively coarse compared to the finest disturbance scales, remains the highest spatial resolution available for dynamical AGC datasets. This improvement facilitates the detection of small-scale disturbance impacts on global carbon dynamics and supports detailed regional analyses.

Our new AGC dataset holds promise for enhancing the representation of carbon cycle processes in land surface and Earth System models. Currently, processes related to disturbances, land-use management, and tree mortality have been either ex-

https://doi.org/10.5194/essd-2025-330
Preprint. Discussion started: 24 July 2025

cluded or poorly represented in these models (Seidl et al., 2011; Manusch et al., 2012; Pongratz et al., 2018; Pugh et al., 2019) due to limited understanding of these processes stemming from a lack of long-term biomass dynamic data. This deficiency contributes to significant uncertainties between Earth system models and satellite-based AGC estimates (Yang et al., 2020a; El Masri and Xiao, 2025). By providing a more comprehensive view of biomass dynamics, our dataset could help reduce these uncertainties, improve predictions of future land carbon sinks, and reconcile divergent estimates of carbon sources and sinks derived from different modeling approaches.

5 Conclusion

We have developed a new long-term, fine spatial resolution global above-ground biomass dataset derived from radar scatter data using a machine learning approach. By incorporating vegetation properties such as tree cover and tree density, as well as background climate variables, our model improves the estimation of above-ground carbon compared to models driven solely by radar scatter data. Our analysis reveals a slight increase in global carbon stocks, characterized by a dynamic balance between AGC gains and losses across different biomes. Temperate and boreal forests are the primary contributors to AGC gains, while AGC losses are predominantly observed in tropical forests, particularly in South America. Interestingly, non-forest ecosystems might contribute to gross carbon gains. Additionally, our dataset captures AGC losses and legacy effects on carbon dynamics resulting from tree mortality. This new dataset can be applied for detecting the complex impacts of disturbances, land-use changes, and extreme events on the global carbon cycle. Furthermore, it has the potential to enhance the representation of these processes in Earth System Models (ESMs), thereby improving the accuracy of future carbon budget.

Code and data availability. The global above-ground biomass dataset at 8 km resolution from 1993 to 2020 is openly available on Zenodo: https://doi.org/10.5281/zenodo.15735548 (Liu et al., 2025). The corresponding modeling code is publicly hosted on GitHub: https://github.com/Guohua-liu/CALIPSO_Biomass/tree/main/AGB_Mapping/scripts.

Author contributions. G.L. and A.B. conceived the research and performed all analyses. S.T. provided support on satellite radar backscatter data analysis, and H.Y. prepared the biomass data from SMOS-IC L-VOD data. G.L. and A.B. performed data processing and interpretation of results. P.C. provided expertise on biomass modeling and assisted with manuscript revisions. All authors contributed to the manuscript and approved the final version.

Competing interests. The authors declare no competing interests.

https://doi.org/10.5194/essd-2025-330
Preprint. Discussion started: 24 July 2025

Acknowledgements. We thank support from the CALIPSO (Carbon Loss in Plant Soils and Oceans) project, funded through the generosity of Eric and Wendy Schmidt by recommendation of the Schmidt Futures program. A.B. acknowledges support from the European Union (ERC StG, ForExD, Grant No. 101039567). We thank Ulrich Weber for data downloading and aggregations.

https://doi.org/10.5194/essd-2025-330
Preprint. Discussion started: 24 July 2025

References

Abatzoglou, J. T., Dobrowski, S. Z., Parks, S. A., and Hegewisch, K. C.: TerraClimate, a high-resolution global dataset of monthly climate and climatic water balance from 1958–2015, Scientific data, 5, 1–12, 2018.

Ahlström, A., Schurgers, G., and Smith, B.: The large influence of climate model bias on terrestrial carbon cycle simulations, Environmental Research Letters, 12, 014 004, 2017.

Allen, C. D., Macalady, A. K., Chenchouni, H., Bachelet, D., McDowell, N., Vennetier, M., Kitzberger, T., Rigling, A., Breshears, D. D., Hogg, E. T., et al.: A global overview of drought and heat-induced tree mortality reveals emerging climate change risks for forests, Forest ecology and management, 259, 660–684, 2010.

Ameray, A., Bergeron, Y., Valeria, O., Montoro Girona, M., and Cavard, X.: Forest carbon management: A review of silvicultural practices and management strategies across boreal, temperate and tropical forests, Current Forestry Reports, pp. 1–22, 2021.

Anderegg, W. R., Hicke, J. A., Fisher, R. A., Allen, C. D., Aukema, J., Bentz, B., Hood, S., Lichstein, J. W., Macalady, A. K., McDowell, N., et al.: Tree mortality from drought, insects, and their interactions in a changing climate, New Phytologist, 208, 674–683, 2015.

Baccini, A., Goetz, S., Walker, W., Laporte, N., Sun, M., Sulla-Menashe, D., Hackler, J., Beck, P., Dubayah, R., Friedl, M., et al.: Estimated carbon dioxide emissions from tropical deforestation improved by carbon-density maps, Nature climate change, 2, 182–185, 2012.

Baccini, A., Walker, W., Carvalho, L., Farina, M., Sulla-Menashe, D., and Houghton, R.: Tropical forests are a net carbon source based on aboveground measurements of gain and loss, Science, 358, 230–234, 2017.

Bastos, A., Friedlingstein, P., Sitch, S., Chen, C., Mialon, A., Wigneron, J.-P., Arora, V. K., Briggs, P. R., Canadell, J. G., Ciais, P., et al.: Impact of the 2015/2016 El Niño on the terrestrial carbon cycle constrained by bottom-up and top-down approaches, Philosophical Transactions of the Royal Society B: Biological Sciences, 373, 20170 304, 2018.

Bastos, A., Ciais, P., Sitch, S., Aragão, L. E. O. C., Chevallier, F., Fawcett, D., Rosan, T. M., Saunois, M., Günther, D., Perugini, L., Robert, C., Deng, Z., Pongratz, J., Ganzenmüller, R., Fuchs, R., Winkler, K., Zaehle, S., and Albergel, C.: On the use of Earth Observation to support estimates of national greenhouse gas emissions and sinks for the Global stocktake process: lessons learned from ESA-CCI RECCAP2, Carbon Balance and Management, 17, 15, https://doi.org/10.1186/s13021-022-00214-w, 2022.

Beer, C., Reichstein, M., Tomelleri, E., Ciais, P., Jung, M., Carvalhais, N., Rödenbeck, C., Arain, M. A., Baldocchi, D., Bonan, G. B., et al.: Terrestrial gross carbon dioxide uptake: global distribution and covariation with climate, Science, 329, 834–838, 2010.

Besnard, S., Santoro, M., Cartus, O., Fan, N., Linscheid, N., Nair, R., Weber, U., Koirala, S., and Carvalhais, N.: Global sensitivities of forest carbon changes to environmental conditions, Global Change Biology, 27, 6467–6483, 2021.

Bonan, G. B.: Forests and climate change: forcings, feedbacks, and the climate benefits of forests, science, 320, 1444–1449, 2008.

Bradley, B. A., Houghton, R., Mustard, J. F., and Hamburg, S. P.: Invasive grass reduces aboveground carbon stocks in shrublands of the Western US, Global Change Biology, 12, 1815–1822, 2006.

Brienen, R. J., Phillips, O. L., Feldpausch, T. R., Gloor, E., Baker, T. R., Lloyd, J., Lopez-Gonzalez, G., Monteagudo-Mendoza, A., Malhi, Y., Lewis, S. L., et al.: Long-term decline of the Amazon carbon sink, Nature, 519, 344–348, 2015.

Burton, P. J., Jentsch, A., and Walker, L. R.: The ecology of disturbance interactions, BioScience, 70, 854–870, 2020.

Bustamante, M. M., Roitman, I., Aide, T. M., Alencar, A., Anderson, L. O., Aragão, L., Asner, G. P., Barlow, J., Berenguer, E., Chambers, J., et al.: Toward an integrated monitoring framework to assess the effects of tropical forest degradation and recovery on carbon stocks and biodiversity, Global change biology, 22, 92–109, 2016.

https://doi.org/10.5194/essd-2025-330
Preprint. Discussion started: 24 July 2025

Crowther, T. W., Glick, H. B., Covey, K. R., Bettigole, C., Maynard, D. S., Thomas, S. M., Smith, J. R., Hintler, G., Duguid, M. C., Amatulli, G., et al.: Mapping tree density at a global scale, Nature, 525, 201–205, 2015.

Dye, A. W., Houtman, R. M., Gao, P., Anderegg, W. R., Fettig, C. J., Hicke, J. A., Kim, J. B., Still, C. J., Young, K., and Riley, K. L.: Carbon, climate, and natural disturbance: a review of mechanisms, challenges, and tools for understanding forest carbon stability in an uncertain future, Carbon Balance and Management, 19, 1–25, 2024.

Eckdahl, J. A., Kristensen, J. A., and Metcalfe, D. B.: Climatic variation drives loss and restructuring of carbon and nitrogen in boreal forest wildfire, Biogeosciences, 19, 2487–2506, 2022.

El Masri, B. and Xiao, J.: Comparison of global aboveground biomass estimates from satellite observations and dynamic global vegetation models, Journal of Geophysical Research: Biogeosciences, 130, e2024JG008 305, 2025.

El-Masri, B., Barman, R., Meiyappan, P., Song, Y., Liang, M., and Jain, A. K.: Carbon dynamics in the Amazonian Basin: Integration of eddy covariance and ecophysiological data with a land surface model, Agricultural and forest meteorology, 182, 156–167, 2013.

Erb, K.-H., Kastner, T., Plutzar, C., Bais, A. L. S., Carvalhais, N., Fetzel, T., Gingrich, S., Haberl, H., Lauk, C., Niedertscheider, M., et al.: Unexpectedly large impact of forest management and grazing on global vegetation biomass, Nature, 553, 73–76, 2018.

Etzold, S., Ferretti, M., Reinds, G. J., Solberg, S., Gessler, A., Waldner, P., Schaub, M., Simpson, D., Benham, S., Hansen, K., et al.: Nitrogen deposition is the most important environmental driver of growth of pure, even-aged and managed European forests, Forest Ecology and Management, 458, 117 762, 2020.

Fan, L., Wigneron, J.-P., Ciais, P., Chave, J., Brandt, M., Fensholt, R., Saatchi, S. S., Bastos, A., Al-Yaari, A., Hufkens, K., et al.: Satellite-observed pantropical carbon dynamics, Nature plants, 5, 944–951, 2019.

Fan, L., Wigneron, J.-P., Ciais, P., Chave, J., Brandt, M., Sitch, S., Yue, C., Bastos, A., Li, X., Qin, Y., et al.: Siberian carbon sink reduced by forest disturbances, Nature Geoscience, 16, 56–62, 2023.

Fan, L., Cui, T., Wigneron, J.-P., Ciais, P., Sitch, S., Brandt, M., Li, X., Niu, S., Xiao, X., Chave, J., et al.: Dominant role of the non-forest woody vegetation in the post 2015/16 El Niño tropical carbon recovery, Global Change Biology, 30, e17 423, 2024.

Fang, H., Fan, L., Ciais, P., Xiao, J., Fensholt, R., Chen, J., Frappart, F., Ju, W., Niu, S., Xiao, X., et al.: Satellite-based monitoring of China's above-ground biomass carbon sink from 2015 to 2021, Agricultural and Forest Meteorology, 356, 110 172, 2024.

Fawcett, D., Sitch, S., Ciais, P., Wigneron, J. P., Silva-Junior, C. H., Heinrich, V., Vancutsem, C., Achard, F., Bastos, A., Yang, H., et al.: Declining Amazon biomass due to deforestation and subsequent degradation losses exceeding gains, Global Change Biology, 29, 1106–1118, 2023.

Feng, Y., Zeng, Z., Searchinger, T. D., Ziegler, A. D., Wu, J., Wang, D., He, X., Elsen, P. R., Ciais, P., Xu, R., et al.: Doubling of annual forest carbon loss over the tropics during the early twenty-first century, Nature Sustainability, 5, 444–451, 2022.

Feng, Y., Ciais, P., Wigneron, J.-P., Xu, Y., Ziegler, A. D., van Wees, D., Fendrich, A. N., Spracklen, D. V., Sitch, S., Brandt, M., et al.: Global patterns and drivers of tropical aboveground carbon changes, Nature Climate Change, 14, 1064–1070, 2024.

Fettig, C. J., Runyon, J. B., Homicz, C. S., James, P. M., and Ulyshen, M. D.: Fire and insect interactions in North American forests, Current Forestry Reports, 8, 301–316, 2022.

Fleta-Soriano, E. and Munné-Bosch, S.: Stress memory and the inevitable effects of drought: a physiological perspective, Frontiers in Plant Science, 7, 143, 2016.

Frank, D., Reichstein, M., Bahn, M., Thonicke, K., Frank, D., Mahecha, M. D., Smith, P., Van der Velde, M., Vicca, S., Babst, F., et al.: Effects of climate extremes on the terrestrial carbon cycle: concepts, processes and potential future impacts, Global change biology, 21, 2861–2880, 2015.

https://doi.org/10.5194/essd-2025-330
Preprint. Discussion started: 24 July 2025

Franklin, J., Serra-Diaz, J. M., Syphard, A. D., and Regan, H. M.: Global change and terrestrial plant community dynamics, Proceedings of the National Academy of Sciences, 113, 3725–3734, 2016.

Friedlingstein, P., O'sullivan, M., Jones, M. W., Andrew, R. M., Bakker, D. C., Hauck, J., Landschützer, P., Le Quéré, C., Luijkx, I. T., Peters, G. P., et al.: Global carbon budget 2023, Earth System Science Data, 15, 5301–5369, 2023.

Friend, A. D., Lucht, W., Rademacher, T. T., Keribin, R., Betts, R., Cadule, P., Ciais, P., Clark, D. B., Dankers, R., Falloon, P. D., et al.: Carbon residence time dominates uncertainty in terrestrial vegetation responses to future climate and atmospheric CO2, Proceedings of the National Academy of Sciences, 111, 3280–3285, 2014.

Fu, Z., Li, D., Hararuk, O., Schwalm, C., Luo, Y., Yan, L., and Niu, S.: Recovery time and state change of terrestrial carbon cycle after disturbance, Environmental Research Letters, 12, 104 004, 2017.

García-Herrera, R., Díaz, J., Trigo, R. M., Luterbacher, J., and Fischer, E. M.: A review of the European summer heat wave of 2003, Critical Reviews in Environmental Science and Technology, 40, 267–306, 2010.

Gatti, L. V., Basso, L. S., Miller, J. B., Gloor, M., Gatti Domingues, L., Cassol, H. L., Tejada, G., Aragão, L. E., Nobre, C., Peters, W., et al.: Amazonia as a carbon source linked to deforestation and climate change, Nature, 595, 388–393, 2021.

Gibbs, H. K. and Ruesch, A.: New IPCC tier-1 global biomass carbon map for the year 2000, Tech. rep., Environmental System Science Data Infrastructure for a Virtual Ecosystem . . . , 2008.

Hammond, W. M., Williams, A. P., Abatzoglou, J. T., Adams, H. D., Klein, T., López, R., Sáenz-Romero, C., Hartmann, H., Breshears, D. D., and Allen, C. D.: Global field observations of tree die-off reveal hotter-drought fingerprint for Earth's forests, Nature Communications, 13, 1761, 2022.

Hansen, M. C., Potapov, P. V., Moore, R., Hancher, M., Turubanova, S. A., Tyukavina, A., Thau, D., Stehman, S. V., Goetz, S. J., Loveland, T. R., et al.: High-resolution global maps of 21st-century forest cover change, science, 342, 850–853, 2013.

Harper, K. L., Lamarche, C., Hartley, A., Peylin, P., Ottlé, C., Bastrikov, V., San Martín, R., Bohnenstengel, S. I., Kirches, G., Boettcher, M., et al.: A 29-year time series of annual 300 m resolution plant-functional-type maps for climate models, Earth System Science Data, 15, 1465–1499, 2023.

Harris, N., Hagen, S., Saatchi, S., Pearson, T., Woodall, C., Domke, G., Braswell, B., Walters, B., Brown, S., Salas, W., et al.: Attribution of net carbon change by disturbance type across forest lands of the conterminous United States, Carbon balance and management, 11, 1–21, 2016.

Hartmann, H., Bastos, A., Das, A. J., Esquivel-Muelbert, A., Hammond, W. M., Martínez-Vilalta, J., McDowell, N. G., Powers, J. S., Pugh, T. A., Ruthrof, K. X., et al.: Climate change risks to global forest health: emergence of unexpected events of elevated tree mortality worldwide, Annual Review of Plant Biology, 73, 673–702, 2022.

Heinrich, V. H., Dalagnol, R., Cassol, H. L., Rosan, T. M., de Almeida, C. T., Silva Junior, C. H., Campanharo, W. A., House, J. I., Sitch, S., Hales, T. C., et al.: Large carbon sink potential of secondary forests in the Brazilian Amazon to mitigate climate change, Nature communications, 12, 1785, 2021.

Heinrich, V. H., Vancutsem, C., Dalagnol, R., Rosan, T. M., Fawcett, D., Silva-Junior, C. H., Cassol, H. L., Achard, F., Jucker, T., Silva, C. A., et al.: The carbon sink of secondary and degraded humid tropical forests, Nature, 615, 436–442, 2023.

Houghton, R., Hall, F., and Goetz, S. J.: Importance of biomass in the global carbon cycle, Journal of Geophysical Research: Biogeosciences, 114, 2009.

Houghton, R. A.: Revised estimates of the annual net flux of carbon to the atmosphere from changes in land use and land management 1850–2000, Tellus B: Chemical and Physical Meteorology, 55, 378–390, 2003.

https://doi.org/10.5194/essd-2025-330
Preprint. Discussion started: 24 July 2025

Hu, T., Su, Y., Xue, B., Liu, J., Zhao, X., Fang, J., and Guo, Q.: Mapping global forest aboveground biomass with spaceborne LiDAR, optical imagery, and forest inventory data, Remote Sensing, 8, 565, 2016.

Hubau, W., Lewis, S. L., Phillips, O. L., Affum-Baffoe, K., Beeckman, H., Cuní-Sanchez, A., Daniels, A. K., Ewango, C. E., Fauset, S., Mukinzi, J. M., et al.: Asynchronous carbon sink saturation in African and Amazonian tropical forests, Nature, 579, 80–87, 2020.

Kannenberg, S. A., Schwalm, C. R., and Anderegg, W. R.: Ghosts of the past: how drought legacy effects shape forest functioning and carbon cycling, Ecology letters, 23, 891–901, 2020.

Konings, A. G., Rao, K., and Steele-Dunne, S. C.: Macro to micro: microwave remote sensing of plant water content for physiology and ecology, New Phytologist, 223, 1166–1172, 2019.

Kwon, M. J., Ballantyne, A., Ciais, P., Bastos, A., Chevallier, F., Liu, Z., Green, J. K., Qiu, C., and Kimball, J. S.: Siberian 2020 heatwave increased spring CO2 uptake but not annual CO2 uptake, Environmental Research Letters, 16, 124 030, 2021.

Lai, L., Huang, X., Yang, H., Chuai, X., Zhang, M., Zhong, T., Chen, Z., Chen, Y., Wang, X., and Thompson, J. R.: Carbon emissions from land-use change and management in China between 1990 and 2010, Science Advances, 2, e1601 063, 2016.

Lauerwald, R., Bastos, A., McGrath, M. J., Petrescu, A. M. R., Ritter, F., Andrew, R. M., Berchet, A., Broquet, G., Brunner, D., Chevallier, F., et al.: Carbon and greenhouse gas budgets of Europe: Trends, interannual and spatial variability, and their drivers, Global Biogeochemical Cycles, 38, e2024GB008 141, 2024.

Lecomte, P. and Wagner, W.: ERS wind scatterometer commissioning and in-flight calibration, EUR SPACE AGENCY SPEC PUBL ESA SP, pp. 261–270, 1998.

Lewis, S. L., Brando, P. M., Phillips, O. L., Van Der Heijden, G. M., and Nepstad, D.: The 2010 amazon drought, Science, 331, 554–554, 2011.

Liu, G., Ciais, Philippe, T. S., Yang, H., and Bastos, A.: A High-Resolution, Long-Term Global Radar-Based Above-Ground Biomass Dataset from 1993 to 2020), https://doi.org/10.5281/zenodo.15735548, 2025.

Liu, S., Bond-Lamberty, B., Hicke, J. A., Vargas, R., Zhao, S., Chen, J., Edburg, S. L., Hu, Y., Liu, J., McGuire, A. D., et al.: Simulating the impacts of disturbances on forest carbon cycling in North America: Processes, data, models, and challenges, Journal of Geophysical Research: Biogeosciences, 116, 2011a.

Liu, Y. Y., De Jeu, R. A., McCabe, M. F., Evans, J. P., and Van Dijk, A. I.: Global long-term passive microwave satellite-based retrievals of vegetation optical depth, Geophysical Research Letters, 38, 2011b.

Liu, Y. Y., Van Dijk, A. I., De Jeu, R. A., Canadell, J. G., McCabe, M. F., Evans, J. P., and Wang, G.: Recent reversal in loss of global terrestrial biomass, Nature Climate Change, 5, 470–474, 2015.

Mack, M. C., Walker, X. J., Johnstone, J. F., Alexander, H. D., Melvin, A. M., Jean, M., and Miller, S. N.: Carbon loss from boreal forest wildfires offset by increased dominance of deciduous trees, Science, 372, 280–283, 2021.

Manusch, C., Bugmann, H., Heiri, C., and Wolf, A.: Tree mortality in dynamic vegetation models–A key feature for accurately simulating forest properties, Ecological Modelling, 243, 101–111, 2012.

Marengo, J. A., Nobre, C. A., Tomasella, J., Oyama, M. D., De Oliveira, G. S., De Oliveira, R., Camargo, H., Alves, L. M., and Brown, I. F.: The drought of Amazonia in 2005, Journal of climate, 21, 495–516, 2008.

Matricardi, E. A. T., Skole, D. L., Costa, O. B., Pedlowski, M. A., Samek, J. H., and Miguel, E. P.: Long-term forest degradation surpasses deforestation in the Brazilian Amazon, Science, 369, 1378–1382, 2020.

McDowell, N. G., Coops, N. C., Beck, P. S., Chambers, J. Q., Gangodagamage, C., Hicke, J. A., Huang, C.-y., Kennedy, R., Krofcheck, D. J., Litvak, M., et al.: Global satellite monitoring of climate-induced vegetation disturbances, Trends in plant science, 20, 114–123, 2015.

https://doi.org/10.5194/essd-2025-330
Preprint. Discussion started: 24 July 2025

Melton, J. R., Chan, E., Millard, K., Fortier, M., Winton, R. S., Martín-López, J. M., Cadillo-Quiroz, H., Kidd, D., and Verchot, L. V.: A map of global peatland extent created using machine learning (Peat-ML), Geoscientific Model Development, 15, 4709–4738, 2022.

Myneni, R. B., Dong, J., Tucker, C. J., Kaufmann, R. K., Kauppi, P. E., Liski, J., Zhou, L., Alexeyev, V., and Hughes, M.: A large carbon sink in the woody biomass of Northern forests, Proceedings of the National Academy of Sciences, 98, 14 784–14 789, 2001.

Olson, D. M., Dinerstein, E., Wikramanayake, E. D., Burgess, N. D., Powell, G. V., Underwood, E. C., D'amico, J. A., Itoua, I., Strand, H. E., Morrison, J. C., et al.: Terrestrial Ecoregions of the World: A New Map of Life on Earth: A new global map of terrestrial ecoregions provides an innovative tool for conserving biodiversity, BioScience, 51, 933–938, 2001.

Pan, Y., Birdsey, R. A., Fang, J., Houghton, R., Kauppi, P. E., Kurz, W. A., Phillips, O. L., Shvidenko, A., Lewis, S. L., Canadell, J. G., et al.: A large and persistent carbon sink in the world's forests, science, 333, 988–993, 2011.

Pan, Y., Birdsey, R. A., Phillips, O. L., and Jackson, R. B.: The structure, distribution, and biomass of the world's forests, Annual Review of Ecology, Evolution, and Systematics, 44, 593–622, 2013.

Pan, Y., Birdsey, R. A., Phillips, O. L., Houghton, R. A., Fang, J., Kauppi, P. E., Keith, H., Kurz, W. A., Ito, A., Lewis, S. L., et al.: The enduring world forest carbon sink, Nature, 631, 563–569, 2024.

Peng, C., Ma, Z., Lei, X., Zhu, Q., Chen, H., Wang, W., Liu, S., Li, W., Fang, X., and Zhou, X.: A drought-induced pervasive increase in tree mortality across Canada's boreal forests, Nature climate change, 1, 467–471, 2011.

Phillips, O. L., Aragão, L. E., Lewis, S. L., Fisher, J. B., Lloyd, J., López-González, G., Malhi, Y., Monteagudo, A., Peacock, J., Quesada, C. A., et al.: Drought sensitivity of the Amazon rainforest, Science, 323, 1344–1347, 2009.

Piao, S., Friedlingstein, P., Ciais, P., Viovy, N., and Demarty, J.: Growing season extension and its impact on terrestrial carbon cycle in the Northern Hemisphere over the past 2 decades, Global Biogeochemical Cycles, 21, 2007.

Pickett, S. T.: Space-for-time substitution as an alternative to long-term studies, in: Long-term studies in ecology: approaches and alternatives, pp. 110–135, Springer, 1989.

Pongratz, J., Dolman, H., Don, A., Erb, K.-H., Fuchs, R., Herold, M., Jones, C., Kuemmerle, T., Luyssaert, S., Meyfroidt, P., et al.: Models meet data: Challenges and opportunities in implementing land management in Earth system models, Global change biology, 24, 1470–1487, 2018.

Pugh, T. A., Arneth, A., Kautz, M., Poulter, B., and Smith, B.: Important role of forest disturbances in the global biomass turnover and carbon sinks, Nature geoscience, 12, 730–735, 2019.

Qin, Y., Xiao, X., Wigneron, J.-P., Ciais, P., Brandt, M., Fan, L., Li, X., Crowell, S., Wu, X., Doughty, R., et al.: Carbon loss from forest degradation exceeds that from deforestation in the Brazilian Amazon, Nature Climate Change, 11, 442–448, 2021.

Reichstein, M., Bahn, M., Ciais, P., Frank, D., Mahecha, M. D., Seneviratne, S. I., Zscheischler, J., Beer, C., Buchmann, N., Frank, D. C., et al.: Climate extremes and the carbon cycle, Nature, 500, 287–295, 2013.

Rodríguez-Fernández, N. J., Mialon, A., Mermoz, S., Bouvet, A., Richaume, P., Al Bitar, A., Al-Yaari, A., Brandt, M., Kaminski, T., Le Toan, T., et al.: An evaluation of SMOS L-band vegetation optical depth (L-VOD) data sets: high sensitivity of L-VOD to above-ground biomass in Africa, Biogeosciences, 15, 4627–4645, 2018.

Saatchi, S. S., Harris, N. L., Brown, S., Lefsky, M., Mitchard, E. T., Salas, W., Zutta, B. R., Buermann, W., Lewis, S. L., Hagen, S., et al.: Benchmark map of forest carbon stocks in tropical regions across three continents, Proceedings of the national academy of sciences, 108, 9899–9904, 2011.

Santoro, M. and Cartus, O.: ESA Biomass Climate Change Initiative (Biomass_cci): Global datasets of forest above-ground biomass for the years 2010, 2017, 2018, 2019 and 2020, v4, (No Title), 2023.

https://doi.org/10.5194/essd-2025-330
Preprint. Discussion started: 24 July 2025

Santoro, M., Cartus, O., Carvalhais, N., Rozendaal, D. M., Avitabile, V., Araza, A., De Bruin, S., Herold, M., Quegan, S., Rodríguez-Veiga, P., et al.: The global forest above-ground biomass pool for 2010 estimated from high-resolution satellite observations, Earth System Science Data, 13, 3927–3950, 2021.

Seidl, R., Fernandes, P. M., Fonseca, T. F., Gillet, F., Jönsson, A. M., Merganičová, K., Netherer, S., Arpaci, A., Bontemps, J.-D., Bugmann, H., et al.: Modelling natural disturbances in forest ecosystems: a review, Ecological modelling, 222, 903–924, 2011.

Shvetsov, E. G., Kukavskaya, E. A., Shestakova, T. A., Laflamme, J., and Rogers, B. M.: Increasing fire and logging disturbances in Siberian boreal forests: A case study of the Angara region, Environmental research letters, 16, 115 007, 2021.

Tagesson, T., Schurgers, G., Horion, S., Ciais, P., Tian, F., Brandt, M., Ahlström, A., Wigneron, J.-P., Ardö, J., Olin, S., et al.: Recent divergence in the contributions of tropical and boreal forests to the terrestrial carbon sink, Nature Ecology & Evolution, 4, 202–209, 2020.

Tao, S., Ao, Z., Wigneron, J.-P., Saatchi, S., Ciais, P., Chave, J., Le Toan, T., Frison, P.-L., Hu, X., Chen, C., et al.: A global long-term, high-resolution satellite radar backscatter data record (1992–2022+): merging C-band ERS/ASCAT and Ku-band QSCAT, Earth System Science Data, 15, 1577–1596, 2023.

Tootchi, A., Jost, A., and Ducharne, A.: Multi-source global wetland maps combining surface water imagery and groundwater constraints, Earth System Science Data, 11, 189–220, 2019.

Tubiello, F. N., Conchedda, G., Wanner, N., Federici, S., Rossi, S., and Grassi, G.: Carbon emissions and removals from forests: new estimates, 1990–2020, Earth System Science Data, 13, 1681–1691, https://doi.org/10.5194/essd-13-1681-2021, 2021.

Tyukavina, A., Hansen, M. C., Potapov, P., Parker, D., Okpa, C., Stehman, S. V., Kommareddy, I., and Turubanova, S.: Congo Basin forest loss dominated by increasing smallholder clearing, Science advances, 4, eaat2993, 2018.

Uribe, M. d. R., Coe, M. T., Castanho, A. D., Macedo, M. N., Valle, D., and Brando, P. M.: Net loss of biomass predicted for tropical biomes in a changing climate, Nature Climate Change, 13, 274–281, 2023.

Vijay, V., Pimm, S. L., Jenkins, C. N., and Smith, S. J.: The impacts of oil palm on recent deforestation and biodiversity loss, PloS one, 11, e0159 668, 2016.

Walker, A. P., De Kauwe, M. G., Bastos, A., Belmecheri, S., Georgiou, K., Keeling, R. F., McMahon, S. M., Medlyn, B. E., Moore, D. J., Norby, R. J., et al.: Integrating the evidence for a terrestrial carbon sink caused by increasing atmospheric CO2, New phytologist, 229, 2413–2445, 2021.

Wang, J. A., Baccini, A., Farina, M., Randerson, J. T., and Friedl, M. A.: Disturbance suppresses the aboveground carbon sink in North American boreal forests, Nature Climate Change, 11, 435–441, 2021.

Wigneron, J.-P., Fan, L., Ciais, P., Bastos, A., Brandt, M., Chave, J., Saatchi, S., Baccini, A., and Fensholt, R.: Tropical forests did not recover from the strong 2015–2016 El Niño event, Science advances, 6, eaay4603, 2020.

Wigneron, J.-P., Li, X., Frappart, F., Fan, L., Al-Yaari, A., De Lannoy, G., Liu, X., Wang, M., Le Masson, E., and Moisy, C.: SMOS-IC data record of soil moisture and L-VOD: Historical development, applications and perspectives, Remote Sensing of Environment, 254, 112 238, 2021.

Williams, C. A., Gu, H., MacLean, R., Masek, J. G., and Collatz, G. J.: Disturbance and the carbon balance of US forests: A quantitative review of impacts from harvests, fires, insects, and droughts, Global and Planetary Change, 143, 66–80, 2016.

Winkler, K., Yang, H., Ganzenmüller, R., Fuchs, R., Ceccherini, G., Duveiller, G., Grassi, G., Pongratz, J., Bastos, A., Shvidenko, A., et al.: Changes in land use and management led to a decline in Eastern Europe's terrestrial carbon sink, Communications Earth & Environment, 4, 237, 2023.

https://doi.org/10.5194/essd-2025-330
Preprint. Discussion started: 24 July 2025

Xu, L., Saatchi, S. S., Yang, Y., Yu, Y., Pongratz, J., Bloom, A. A., Bowman, K., Worden, J., Liu, J., Yin, Y., et al.: Changes in global terrestrial live biomass over the 21st century, Science Advances, 7, eabe9829, 2021.

Yang, H., Ciais, P., Santoro, M., Huang, Y., Li, W., Wang, Y., Bastos, A., Goll, D., Arneth, A., Anthoni, P., et al.: Comparison of forest above-ground biomass from dynamic global vegetation models with spatially explicit remotely sensed observation-based estimates, Global Change Biology, 26, 3997–4012, 2020a.

Yang, H., Ciais, P., Frappart, F., Li, X., Brandt, M., Fensholt, R., Fan, L., Saatchi, S., Besnard, S., Deng, Z., et al.: Global increase in biomass carbon stock dominated by growth of northern young forests over past decade, Nature Geoscience, 16, 886–892, 2023.

Yang, L., Liang, S., and Zhang, Y.: A new method for generating a global forest aboveground biomass map from multiple high-level satellite products and ancillary information, IEEE Journal of Selected Topics in Applied Earth Observations and Remote Sensing, 13, 2587–2597, 2020b.

Yang, Y., Saatchi, S. S., Xu, L., Yu, Y., Choi, S., Phillips, N., Kennedy, R., Keller, M., Knyazikhin, Y., and Myneni, R. B.: Post-drought decline of the Amazon carbon sink, Nature Communications, 9, 3172, 2018.

Yang, Y., Saatchi, S., Xu, L., Keller, M., Corsini, C. R., Aragão, L. E., Aguiar, A. P., Knyazikhin, Y., and Myneni, R. B.: Interannual variability of carbon uptake of secondary forests in the Brazilian Amazon (2004-2014), Global Biogeochemical Cycles, 34, e2019GB006 396, 2020c.

Yao, L., Liu, T., Qin, J., Jiang, H., Yang, L., Smith, P., Chen, X., Zhou, C., and Piao, S.: Carbon sequestration potential of tree planting in China, Nature Communications, 15, 8398, 2024.

Yu, Y. and Saatchi, S.: Sensitivity of L-band SAR backscatter to aboveground biomass of global forests, Remote sensing, 8, 522, 2016.